Magnetic and optical properties of electrodeposited nanospherical copper doped nickel oxide thin films

Rufus O. Ijeh[a,b], Assumpta C. Nwanya[b,c,d], Agnes C. Nkele[b], Itani G. Madiba[c,d], Z. Khumalo[c], A.K.H. Bashir[c,d], R.U. Osuji[b,c,d], M. Maaza[c,d], Fabian I. Ezema[b,c,d,e,*]

[a] Science Education Department, College of Education, Agbor, Nigeria
[b] Department of Physics and Astronomy, University of Nigeria, Nsukka, Nigeria
[c] Nanosciences African Network (NANOAFNET) iThemba LABS-National Research Foundation, 1 Old Faure Road, Somerset West, 7129, P.O. Box 722, Somerset West, Western Cape Province, South Africa
[d] UNESCO-UNISA Africa Chair in Nanosciences/Nanotechnology, College of Graduate Studies, University of South Africa (UNISA), Muckleneuk Ridge, P. O. Box 329, Pretoria, South Africa
[e] Department of Physics, Faculty of Natural and Applied Sciences, Coal City University, Enugu, Nigeria

ARTICLE INFO

ABSTRACT

Copper doped nickel oxide (NiO:Cu) thin films were synthesized via electrodeposition technique. X-ray diffraction, Scanning Electron Microscope, UV–visible spectroscopy, Vibrating Sample Magnetometer techniques and electrochemical analysis were utilized for the study of the structural, morphological, optical, magnetic and cyclic voltammogram properties respectively of both undoped and doped NiO thin films. The crystallographic studies of the undoped and doped NiO thin films showed that they are polycrystalline with cubic structure. Surface morphology of both the undoped and doped thin films showed nanocrystalline grains with spherical shaped particles. The optical studies showed a decrease in band gap energy from 3.34 eV to 3.32 eV and finally to 3.20 eV for the undoped, 2% and 3% respectively. The refractive index peaked between 2.60 and 2.65 while the calculated extinction coefficient values of the doped thin films have significant variation in the visible and NIR range. The studies of magnetization saturation values were found to be 1.52E-4 and 2.29E-4 for 2% and 3% doped respectively with low remanence values. Electrochemical studies revealed good cyclic voltammograms of the deposited films. These values indicate that the electrodeposited Cu doped NiO thin films are good candidates for magnetic applications.

1. Introduction

There is tremendous effort in researches towards the development of materials that can ultimately enhance storage of data in computers in form of non-volatile memory [1]. This has provided much interest in the study of the magnetic properties of nanomaterials as they ultimately allow manipulation of electronic charge and spin by controlling the magnetic field [2]. It is obvious that the bulk antiferromagnetic materials have zero net magnetic moment in zero applied fields while fine particles of same material display either super-paramagnetism or weak ferromagnetism [3].

Nickel oxide (NiO) is one of the important transition metals oxides that possesses interesting optical, electronic and magnetic properties with novel morphologies as a result of large number of spins and surface atoms [4–7]. NiO has a rock-salt structure and exhibits a natural antiferromagnetic behavior with magnetic moments inhabiting on Ni^+ ions. NiO nanoparticle is a p-type semiconductor with wide band gap in the range of 3.6 eV–4.0 eV [8,9]. The low resistivity exhibited by NiO has given researchers much concern [10]. In order to circumvent this challenge especially in this technologically driven era, hence the need for doping of NiO nanomaterials arises.

Interestingly, doping of NiO with any of these transition metals (Cu, Fe, Au or Li) changes its optical, electronic and magnetic properties creating Diluted Magnetic Semiconductor (DMS) as a result of spin degrees of freedom and hole content which enhances its application in spintronics [4,8,11]. NiO nanoparticle is a prominent magnetic material that exhibits interesting behavior with applications in the magnetic recording, spin valves, magnetic random access memories, energy transformation, magnetocaloric refrigeration and ferrofluid technology [12–15]. Manouchehri et al. [16], investigated Cu-doped NiO using RF
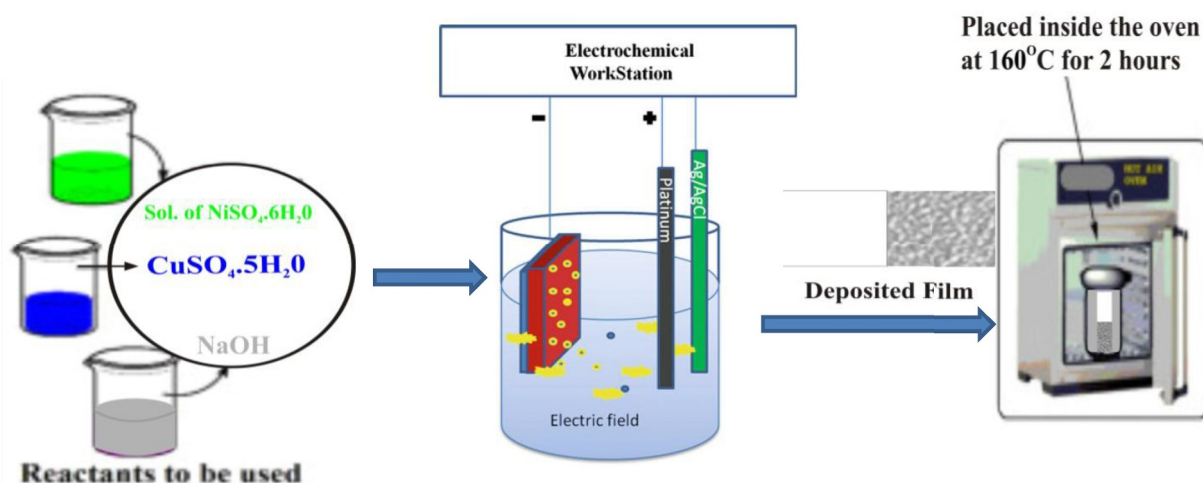

Fig. 1. Systematic representation of undoped and NiO:Cu thin films deposited by electrodeposition method.

magnetron sputtering deposition technique and found that by increasing the Cu dopant percentage, the crystal structure decreased tending to amorphous structure, and the energy band gap values also decreased. Rahdar et al. [17], investigated copper doped NiO nanoparticles using chemical method and the XRD showed that the structure is face centered cubic. The magnetization property studied shows weak ferromagnetism. Zhao et al. [18], investigated the optical and electrochemical properties of Cu-doped NiO thin films synthesized by electrochemical deposition. The films were amorphous and the grains showed a tinge of face-centered cubic. Malllick et al. [19], studied the magnetic behavior of Fe doped NiO and found that NiO nanocrystals show magnetic properties due to increase in Fe doping. Nair et al. [20], studied the structure and magnetic behavior of Mn and Sn -doped NiO using a sol-gel technique. Their results showed that Mn and Sn have no effect on the crystallographic arrangement of NiO thin films. They also found that doped Mn–NiO and pure NiO thin films exhibited ferromagnetic behavior while Sn doped NiO samples showed superparamagnetism.

NiO thin films could be applied in dye-sensitized solar cells, organic light emitting diodes, electrodes in electrochromic devices for developing chemical sensors [21–25]. The deposition techniques used by numerous researchers for the synthesis of NiO thin films include SILAR [26], solution growth [27], chemical vapor deposition [28], spray pyrolysis [26], chemical bath [29] and DC reactive sputtering [30]. It is plausible that of all these deposition methods, electrochemical deposition is simplistic and quite potent for industrial applications as a result of its cost effectiveness and environmental friendliness. High purity films can also be easily obtained at room temperature using this technique. Hence, we synthesized Cu doped NiO thin films using electrodeposition technique. We studied the morphological, optical, magnetic and electrochemical properties of the deposited thin films. It is worth mentioning here that from our literature survey this is the first time that the magnetic properties of Cu doped NiO thin films deposited by electrochemical technique is studied.

2. Experimental details

It is expedient to say that highly purified chemicals were used in this work. Thin films of NiO doped with Cu were prepared using electrochemical method. The ITO coated substrates were incised into 2.5 cm × 1.0 cm dimensions and washed with detergent. The substrates were consequently cleaned with deionized water, rinsed with acetone and desiccated in air for two hours. In order to prepare NiO nanoparticles, 100 ml of 0.05 M of nickel sulphate ($NiSO_4 \cdot 6H_2O$) aqueous solution as Ni source was prepared and 100 ml of 1 M NaOH solution

was added to the above solution at room temperature. Also prepared was 2 and 3 wt % of copper for the doping using copper sulphate pentahydrate solution ($CuSO_4 \cdot 5H_2O$) as Cu source and added to 100 ml of 0.05 M nickel sulphate solution at room temperature. The pH was adjusted to 9 using sodium hydroxide as a precipitator agent. The electrochemical deposition was carried out in a three electrode chamber made up of a silver-silver chloride (Ag/AgCl) electrode serving as reference electrode, carbon rod as anode, and working electrode acting as cathode. At room temperature, a cathodic deposition of Cu-doped NiO was carried for 2 min under potentiostatic condition with a dc voltage of 10 V. X-ray diffraction (XRD) patterns were employed in order to identity the crystallographic phases in the 2θ interval from 10° to 90° using Philips diffractometer model PW1800. The scanning electron microscope (SEM) model JSM 35 CF JEOL was used to probe the surface morphology of the fabricated thin films. A double beam UV-VIS spectrophotometer was used to obtain absorbance spectrum of the thin films in the wavelength range of 300 nm–1000 nm. Furthermore, a vibrating sample magnetometer (VSM) [Lake Shore Model 7404] was also used for the magnetization readings while the Cyclic voltammogram of the deposited films was carried out using a conventional three-electrode connected to autolab instrument (Metrohm) system. A schematic representation of the electrodeposition apparatus for the synthesis of the undoped and NiO:Cu thin films is shown in Fig. 1.

3. Results and discussion

3.1. Structural properties

The x-ray diffraction (XRD) patterns of the undoped and Cu doped NiO thin films (2 and 3%) are shown in Fig. 2. It is observed from the XRD crystallographic structure that both the undoped and doped samples exhibited diffraction peaks which belonged to tin oxide that comes from the FTO-coated glass substrates, which created a strong distortion of the lattice in our case due to F doping of the SnO_2 as suggested by Zhao et al. [18] (in their case they observed weak distortion). The diffraction peaks were seen along the (101), (200), (211) and (310) planes (JCPDS 46-1088). The weak diffraction peaks observed for the doped samples along the (111) and (200) planes belong to the face-centered cubic $Ni_xCu_{1-x}O$ (JCPDS 78-0648) which are as a result of the nanosphere as seen from the SEM as opposed to nanorods observed by Zhao et al. [18]. Doping NiO with Cu increased the crystalline nature of the films and the size of the nanoparticles seen as from the SEM images in Fig. 3. This is in agreement with the results obtained by Zhao et al. [18]. Furthermore, the crystallographic structure suggests that the undoped and Cu doped NiO thin films were
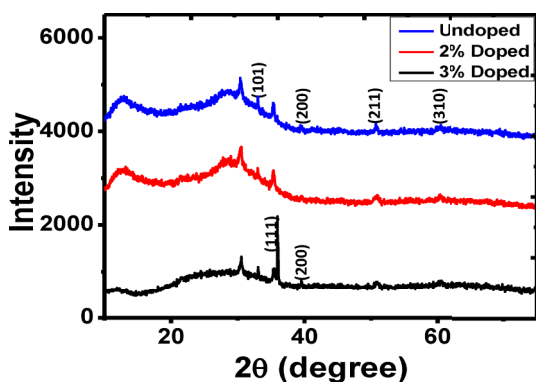
Fig. 2. XRD patterns of undoped NiO and NiO:Cu thin films.

polycrystalline with cubic structure which is in agreement with the works of Kim et al. and other authors [31–33].

It is evidenced that the peak positions for both undoped NiO and Cu doped NiO thin films are the same which is consistent with the works of Manouchehria et al. [16] and others [33,34]. This is because the ionic radii of copper (0.96 Å) is almost the same as that of nickel (0.78 Å), hence the easy substitution of Cu^+ for Ni^+ ions without distortion of the crystal lattice. The crystallite sizes calculated using Schrerrer's formula [34–36] were 35.97 nm for the undoped while 2 and 3% doped NiO thin films were 30.55 nm and 30.38 nm respectively as shown in Table 1. The observed reduction of particle size may be due to defect and disorder of NiO lattice. The works of Malllick et al. [19], on Fe-doped NiO also shows similar reduction in grain size as the dopant level increased

$$D = \frac{k\lambda}{\beta cos\theta} \qquad (1)$$

where k is a dimensionless shape factor β, is the line broadening at half the maximum intensity (FWHM) and λ being the x-ray wavelength and θ as the Bragg angle.

3.2. Surface morphology

The scanning electron microscopy images for the undoped and Cu doped NiO thin films are shown in Fig. 3(a)–(c). The micrograph reveals that both undoped and doped NiO thin films are made of nanocrystalline grains. The surface micrograph of the undoped NiO thin film has uniform distribution of structured grains as shown in Fig. 3(a). There is evidence of homogeneous, spherical, dense, devoid of cracks indicating adhesiveness of grains to the substrate as seen in Fig. 3(b) and (c). A close look at the doped thin films shows that the 3% doped thin film shown in Fig. 3(c) has larger grains with the same magnification of 100X.
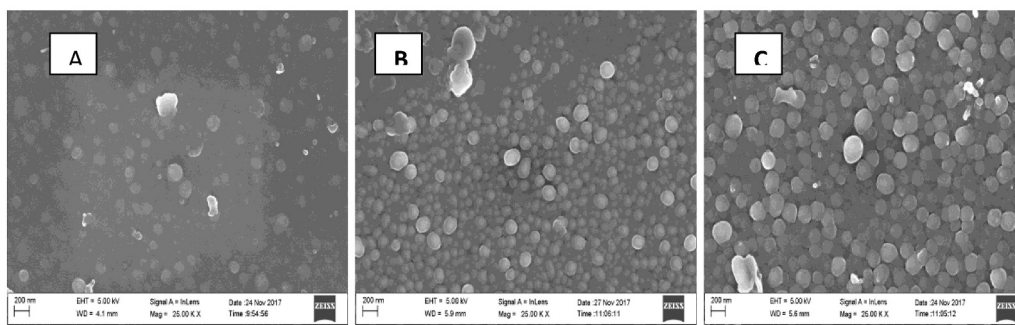
Table 1
Calculated crystallite size, refractive index and energy band gap of the deposited films.

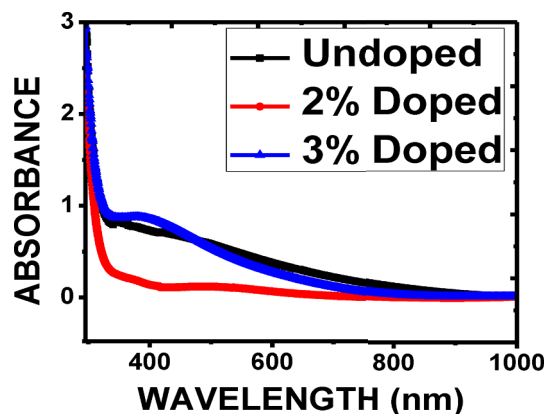| Samples	Crystallite size (nm)	Refractive index	Energy bandgap (eV)
Undoped	35.97	2.30	3.34
2% Doped	30.55	2.30	3.32
3% Doped	30.38	2.60	3.20

Fig. 4. Absorbance versus wavelength plot for the undoped and NiO:Cu thin films.

3.2.1. Optical absorbance

Fig. 4 represents a plot of absorbance of undoped and Cu doped NiO thin films versus wavelength. The absorption spectra of the films deposited on the ITO substrate were investigated at room temperature. The absorbance of the undoped NiO thin film was found to decay exponentially from 100 to 40%, then gradually decreased to 35% and remained fairly constant from 500 nm wavelength to near infra red. The 2% copper doped NiO thin film decreased exponentially from 100 to 72% at wavelength of 300 nm–327 nm, then increased to 75% at 382 nm and later decreased gradually. Also the 3% copper doped NiO thin film exponentially decreased from 100 to 70% at wavelength range of 300–345 nm, thereafter decreased gradually. It is seen that the undoped film has lower absorbance than Cu doped NiO thin films. However, dopant variation was not significantly noticed in the doped samples as they have similar absorbance property.

3.2.2. Transmittance

For optical systems, the transmittance is determined by the optical resistance, quality of the film and surface roughness that scatter light which has to be controlled under normal condition. The transmittance of undoped NiO and Cu doped NiO thin films are presented in Fig. 5. It is noticed that at 450 nm, the undoped increased rapidly to 72.90% while the recorded transmittance values for the doped thin films are
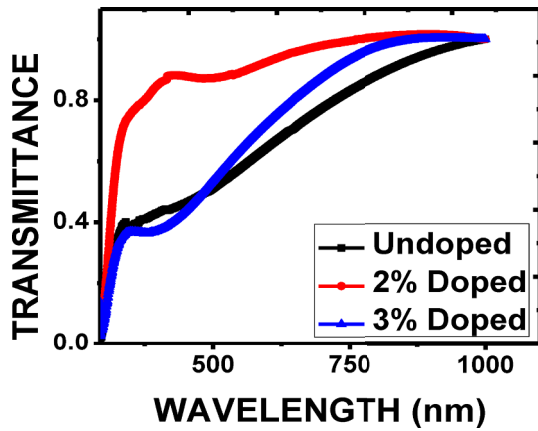

Fig. 3. SEM images of a) undoped NiO b) 2% doped and c) 3% doped NiO:Cu thin films.

Fig. 5. Transmittance profile versus wavelength for the deposited films.

31.34%. However, beyond this value, the 3% transmits more than the 2% although all converge in the infra red region.

3.2.3. Reflectance spectra

The reflectance profile for the undoped and Cu doped NiO thin films versus wavelength is presented in Fig. 6. The reflectance of undoped thin film was 14% at 340 nm which decreases exponentially as wavelength increased. The Cu-doped NiO (2 and 3%) thin films were found to be 20% at 340 nm respectively and remained constant up to 490 nm, thereafter decreased as wavelength increased. Notably, the effect of doping is seen in the doped thin films. Considering T as the Transmittance and A as the absorbance of the film then, the reflectance of the film can be deduced using the relationship:

$$A + R + T = 1 \tag{2}$$

$$R = 1 - (A + T) \tag{3}$$

3.2.4. Optical band gap

A variation of absorption coefficient against the photon energy gives the optical band gap (E_g) of thin films which can be determined using Tauc's relation [32]:

$$(\alpha h\nu)^2 = A(h\nu - E_g)^n \tag{4}$$

where A is the absorption coefficient, hν being the photon energy, E_g is the band gap and n = 1/2 for allowed direct transition or 2 for indirect inter band transitions. The band gap of thin films is obtained by drawing a straight-line tangent to the point on the photon energy axis in which the absorption coefficient is zero as shown in Fig. 7. The band gaps for the undoped NiO, Cu doped NiO (2 and 3%) thin films are 3.34,
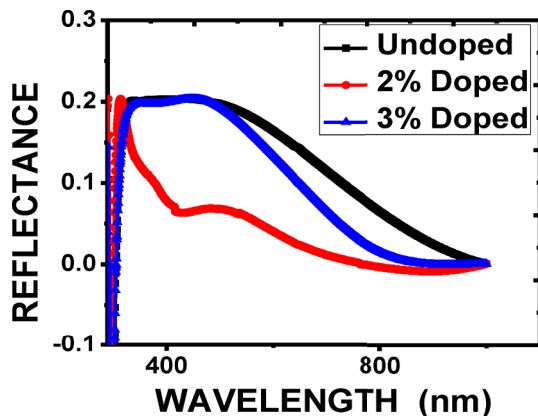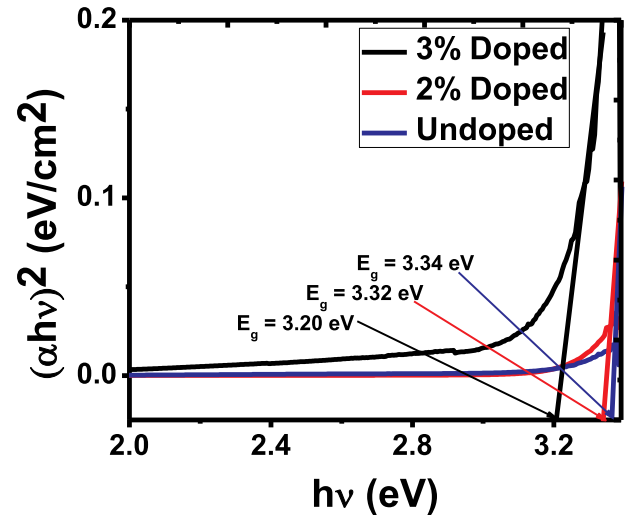

Fig. 7. Plot showing the optical band gaps of the undoped and doped NiO:Cu thin films.

3.32 and 3.20 eV respectively. The decrease in energy bandgap from 3.34 to 3.20 eV may be due to increase in the width of donor levels of copper atoms [16,34]. The obtained band gap values agree with the works of Rahdar et al. [17]. The linear plot obtained for the undoped, 2 and 3% doped NiO thin films indicates that they have direct band gap and are semiconductors.

3.2.5. Refractive index

A variation of refractive index with photon energy of undoped NiO and Cu-doped NiO of (2 and 3%) thin films is presented in Fig. 8. The refractive index was determined by using the following relationship [37]:

$$n = \frac{1 + \sqrt{R}}{1 - \sqrt{R}} \tag{5}$$

where n is the refractive index, R is the reflectance.

It is observed that the refractive index increases rapidly at 300 nm and then peaked at 2.60 for the undoped while the 2% peaked at 2.65 and 3% peaked at 2.60. The effect of doping on refractive index was noticed on the 3% doped as recorded in Table 1. The refractive index of the films ranged from about 2.60 to 2.65 in the visible region of the electromagnetic spectrum. This result is consistent with other reports [38].
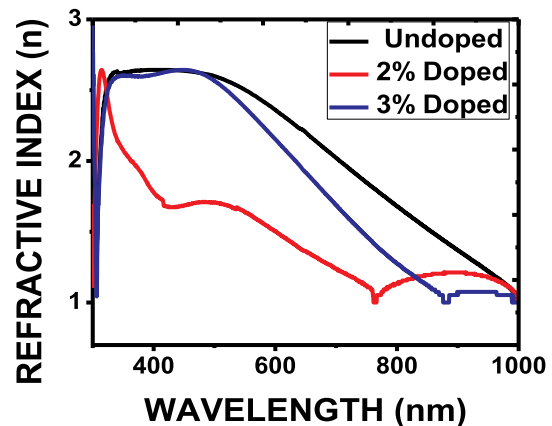

Fig. 6. Reflectance profile versus wavelength for the undoped and the doped NiO thin films.

Fig. 8. Plot showing the variation of refractive index versus photon energy for the films.
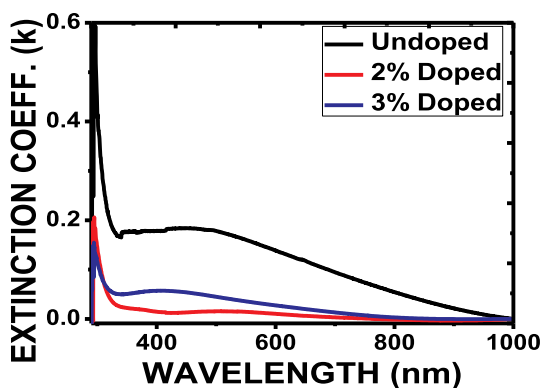
Fig. 9. Plot of extinction coefficient versus photon energy for the deposited films.

3.2.6. Extinction coefficient

This is the measurement of the degree of diminution of light at a given wavelength. The extinction coefficient of the films can be calculated using Eq. (6) [39]:

$$k = \frac{\alpha\lambda}{4\pi} \tag{6}$$

where k is the extinction coefficient, λ is the wavelength of the incident photon and α, the absorption coefficient. It is shown from Eq. (6) that the extinction coefficient varies proportionately with absorption coefficient. From the graph of extinction coefficient against wavelength shown in Fig. 9, it is noticeable that the extinction coefficient of the undoped sample recorded a higher value as compared to that of the doped films due to lack of Cu^+ in the Ni^+ lattice.

3.2.7. Dielectric constants

The real part of complex dielectric constant (ε_r) is a measure of how the speed of light is reduced in a medium and it is often related to the n value, while the imaginary part (ε_i) deals with loss of energy into the medium. Fig. 10(a) and (b) depict the variation of the real and imaginary parts of the dielectric constant values versus wavelength. The values of ε_r and ε_i were determined using Eqs. (7) and (8) respectively [39]. The Cu doped NiO thin films (2 and 3%) increased proportionately and attained higher ε_r values towards increasing wavelength regions than the undoped film as seen in Fig. 10 (a). Fig. 10(b) shows a gradual decrease in the ε_i value of the undoped film as it tends towards the infrared region as compared to the doped films.

$$\varepsilon_r = n^2 - k^2 \tag{7}$$

$$\varepsilon_i = 2nk \tag{8}$$

3.3. Magnetic properties

The magnetic behavior of NiO nanoparticles was studied by plotting the magnetic moment against applied magnetic field using a VSM technique. Fig. 11 (a) shows the hysteresis loop of undoped NiO sample recorded at fields of −400 and 400 Oe at room temperature which depicts some elements of diamagnetism ordering due to quantum mechanical effect creating opposing magnetic field [40]. The emergence of hysteresis curve shown in Fig. 11(b) depicts the ferromagnetic ordering in the doped samples. The substitution of Cu^{2+} for Ni^{2+} together with the presence of a moderate oxygen vacancy can be attributed to the condition of ferromagnetism. The magnetization saturation value (Ms) for the 2% doped was 1.52E-4 emu/g while for the 3% Cu doped the value increased to 2.29E-4 emu/g. The reduction of particle size as shown on Table 1 due to increase in Cu dopant level from 2 to 3% results in enhancement of the magnetic structure as shown in Fig. 11(b). Furthermore, it is evident that the magnetic properties of both undoped NiO, Cu doped NiO (2 and 3%) thin films correspond with magnetic materials of sizes greater than 10 nm [17,41–43]. The saturation magnetization values for the magnetic samples shown in Fig. 11 (b) depends on the Cu content in NiO, which is less than that of the NiO bulk materials (55 emu/g) [41,42]. Hence, magnetization progresses from domain wall to magnetization rotation for the Cu doped NiO thin films thereby leading to increase in coercive force from 40.24 to 55.99 [44]. Also the calculated squareness values obtained for the 2 and 3% doped samples are 0.012 and 0.0844 respectively. The coercive force of the undoped has negative value compared with the doped samples as shown on Table 2.

3.4. Electrochemical properties

The electrochemical properties of the doped and undoped NiO thin films were measured using cyclic voltammogram (CV) in 0.5 M sodium hydroxide as electrolyte at a potential window of 0.1–0.6 V potential range using satd. Ag/AgCl as reference electrode and platinum wire as counter electrode while the NiO thin films on stainless steel substrate serve as the working electrodes.

Fig. 12 (a) shows the comparison of cyclic voltammetry of the various films. The undoped NiO film gave no obvious redox peaks while the doped films gave pronounced redox peaks implying that substitution of some of the Ni ions with Cu ions increased the redox activities of the thin films. While the 3% doped showed redox peaks centered at 0.43/0.53 V/Ag/AgCl, the 2% doped showed a cathodic peak at 0.44 V/Ag/AgCl. The redox peaks current increases with increase in scan rates (Fig. 12(b and c, and d)), an indication that the redox processes are mainly due to intercalation and de-intercalation of ions into the matrix of the thin films [45]. While the anodic peak shifts slightly to the more positive potential, the cathodic peak shifts to the more negative potential an indication of quasi reversible nature of the redox processes

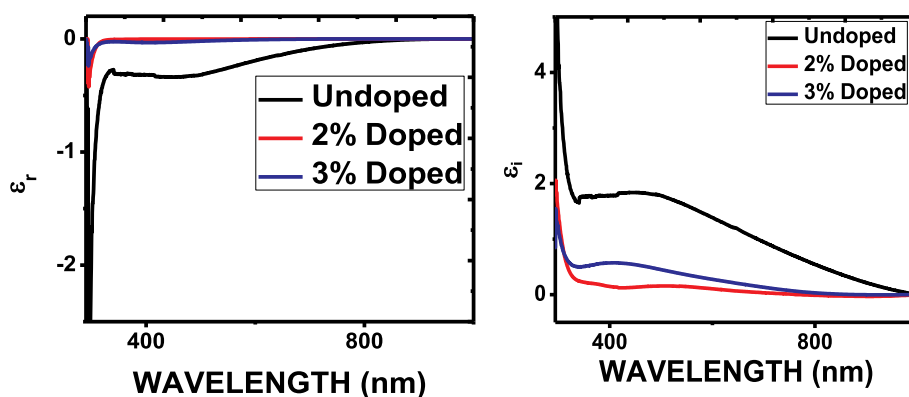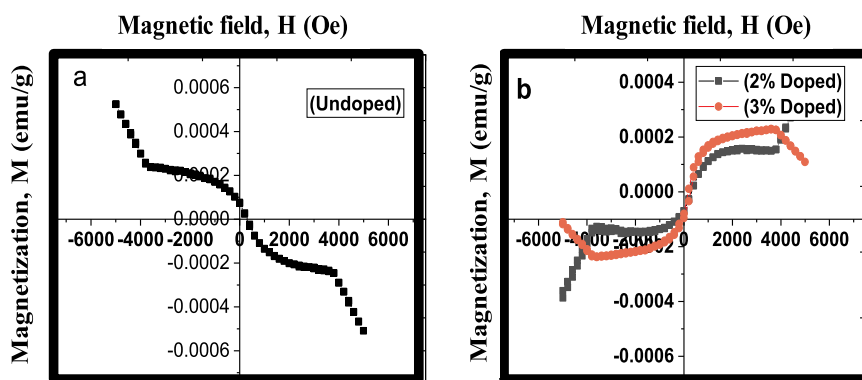**Fig. 10.** Plots of a) real dielectric constant versus wavelength b) imaginary dielectric constant versus wavelength for the deposited films.

Fig. 11. (a): M-H curve of undoped NiO thin film (b) M-H curve of NiO:Cu thin films.

Table 2
Magnetization of undoped and NiO:Cu thin films.

Sample	Magnetization saturation	Coercive field	Remnant magnetization	HOₑ
Undoped	−2.38E-4	−0.50	8.30E-7	4000
2% Doped	1.52E-4	40.24	1.83E-5	4000
3% Doped	2.29E-4	55.99	2.11E-5	4000

due to increase in the internal resistance of the electrode [46]. The anodic scan causes the oxidation of Ni^{2+} to Ni^{3+} while the reduction of the Ni^{3+} to Ni^{2+} takes place during the reverse cathodic scan.

4. Conclusion

In this work, copper was doped on NiO at 0, 2 and 3% using electrodeposition method. The structural, optical and magnetic properties of the thin films were studied using X-ray diffraction, scanning electron microscope, UV–visible spectroscopy, Vibrating Sample Magnetometer and cyclic voltammetric techniques. The doped thin films were polycrystalline and cubic in nature with spherical shaped grains. The transmittance for the undoped was 80% while the doped films in the visible range spectrum lies within the range of 60–70%. The reflectance for the undoped was 14% and the doped was 20% at 340 nm. It was also observed that as the doping percentage increased, the energy band gap reduced significantly. The magnetization saturation and coercive field values for the 2 and 3% doped thin films are quite larger than the undoped film. Electrochemical studies showed good cyclic voltammograms of the deposited films. This result shows that the electrodeposited Cu doped NiO thin films have good potentials for magnetic applications.
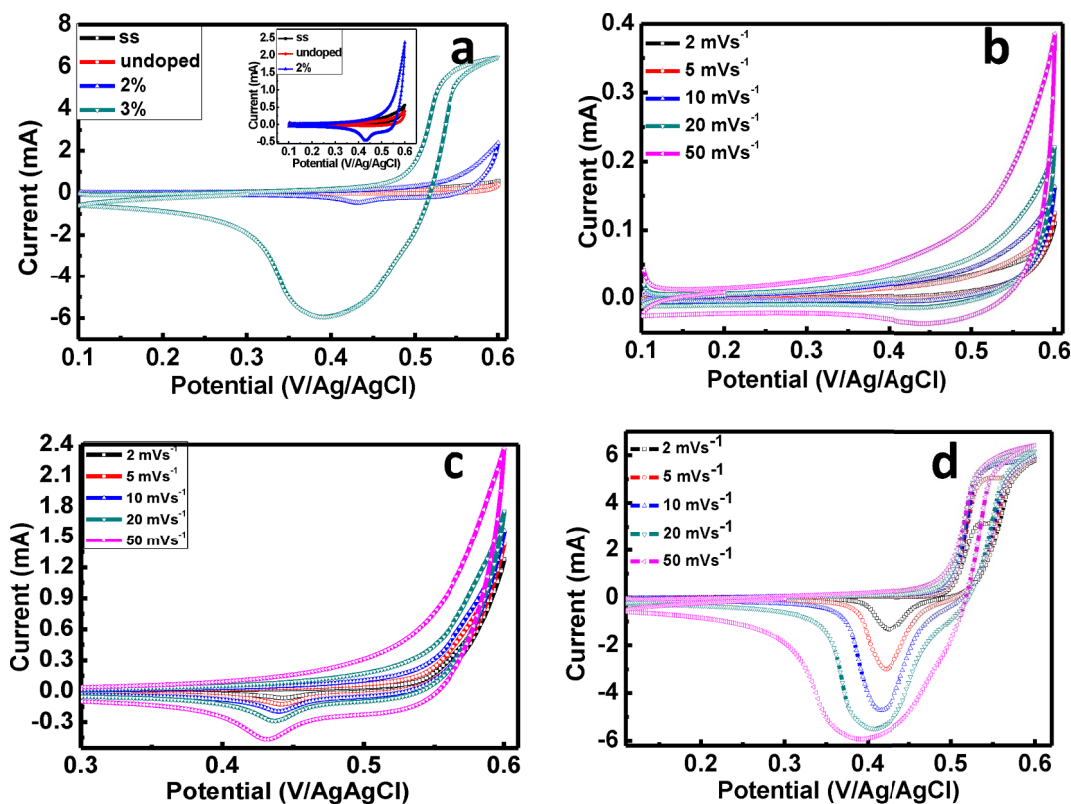
Fig. 12. (a) CV of the doped and undoped NiO films at 50 mVs⁻¹; CVs at various scan rates (b) undoped, (c) 2% doped (d) 3% doped NiO thin films.

References

[1] H. Alameer, U. Kang, K.E. Criss, R. Agarwal, W. Wu, J.B. Halbert, Stacked memory chip device with enhanced data protection capability, US20190004909A1, 2019. https://patents.google.com/patent/US20190004909A1/en (accessed April 9, 2019).

[2] H.S. Nalwa, Encyclopedia of Nanoscience and Nanotechnology vol. 10, American Scientific Publishers, 2004, http://125.234.102.146:8080/dspace/handle/DNULIB_52011/4815 (accessed April 8, 2019).

[3] Z.-Y. Chen, Y. Chen, Q.K. Zhang, X.Q. Tang, D.D. Wang, Z.Q. Chen, P. Mascher, S.J. Wang, Vacancy-induced ferromagnetic behavior in antiferromagnetic NiO nanoparticles: a positron annihilation study, ECS J. Solid State Sci. Technol. 6 (2017) P798–P804, https://doi.org/10.1149/2.0081712jss.

[4] R.H. Kodama, S.A. Makhlouf, A.E. Berkowitz, Finite size effects in antiferromagnetic NiO nanoparticles, Phys. Rev. Lett. 79 (1997) 1393–1396, https://doi.org/10.1103/PhysRevLett.79.1393.

[5] E. Winkler, R.D. Zysler, M.V. Mansilla, D. Fiorani, Surface anisotropy effects in NiO nanoparticles, Phys. Rev. B 72 (2005) 132409, https://doi.org/10.1103/PhysRevB.72.132409.

[6] N. Wang, H. Song, H. Ren, J. Chen, M. Yao, W. Huang, W. Hu, S. Komarneni, Partly nitrogenized nickel oxide hollow spheres with multiple compositions for remarkable electrochemical performance, Chem. Eng. J. 358 (2019) 531–539, https://doi.org/10.1016/j.cej.2018.10.079.

[7] T. Abzieher, S. Moghadamzadeh, F. Schackmar, H. Eggers, F. Sutterlüti, A. Farooq, D. Kojda, K. Habicht, R. Schmager, A. Mertens, R. Azmi, L. Klohr, J.A. Schwenzer, M. Hetterich, U. Lemmer, B.S. Richards, M. Powalla, U.W. Paetzold, Electron-beam-evaporated nickel oxide hole transport layers for perovskite-based photovoltaics, Adv. Energy Mater. 9 (2019) 1802995, https://doi.org/10.1002/aenm.201802995.

[8] J. Wang, J. Cai, Y.-H. Lin, C.-W. Nan, Room-temperature ferromagnetism observed in Fe-doped NiO, Appl. Phys. Lett. 87 (2005) 202501, https://doi.org/10.1063/1.2130532.

[9] H. Gleiter, Nanostructured materials: basic concepts and microstructure, Acta Mater. 48 (2000) 1–29, https://doi.org/10.1016/S1359-6454(99)00285-2.

[10] P.A.L. Sheena, A. Sreedevi, C. Viji, V. Thomas, Nickel oxide/cobalt phthalocyanine nanocomposite for potential electronics applications, Eur. Phys. J. B 92 (2019) 13, https://doi.org/10.1140/epjb/e2018-90280-8.

[11] E. Avendaño, A. Azens, G.A. Niklasson, C.G. Granqvist, Electrochromism in nickel oxide films containing Mg, Al, Si, V, Zr, Nb, Ag, or Ta, Sol. Energy Mater. Sol. Cell. 84 (2004) 337–350, https://doi.org/10.1016/j.solmat.2003.11.032.

[12] M.E. McHenry, D.E. Laughlin, Nano-scale materials development for future magnetic applications, Acta Mater. 48 (2000) 223–238, https://doi.org/10.1016/S1359-6454(99)00296-7.

[13] I. Žutić, J. Fabian, S. Das Sarma, Spintronics: fundamentals and applications, Rev. Mod. Phys. 76 (2004) 323–410, https://doi.org/10.1103/RevModPhys.76.323.

[14] S.A. Wolf, D.D. Awschalom, R.A. Buhrman, J.M. Daughton, S. von Molnár, M.L. Roukes, A.Y. Chtchelkanova, D.M. Treger, Spintronics: a spin-based electronics vision for the future, Science 294 (2001) 1488–1495, https://doi.org/10.1126/science.1065389.

[15] G.A. Prinz, Magnetoelectronics, Science 282 (1998) 1660–1663, https://doi.org/10.1126/science.282.5394.1660.

[16] I. Manouchehri, D. Mehrparvar, R. Moradian, K. Gholami, T. Osati, Investigation of structural and optical properties of copper doped NiO thin films deposited by RF magnetron reactive sputtering, Optik 127 (2016) 8124–8129, https://doi.org/10.1016/j.ijleo.2016.06.005.

[17] A. Rahdar, M. Aliahmad, Y. Azizi, Synthesis of Cu doped NiO nanoparticles by chemical method, J. Nanostruct. 4 (2014) 145–152, https://doi.org/10.7508/jns.2014.02.003.

[18] L. Zhao, G. Su, W. Liu, L. Cao, J. Wang, Z. Dong, M. Song, Optical and electrochemical properties of Cu-doped NiO films prepared by electrochemical deposition, Appl. Surf. Sci. 257 (2011) 3974–3979, https://doi.org/10.1016/j.apsusc.2010.11.160.

[19] P. Mallick, C. Rath, R. Biswal, N.C. Mishra, Structural and magnetic properties of Fe doped NiO, Indian J. Phys. 83 (2009) 517–523, https://doi.org/10.1007/s12648-009-0012-4.

[20] L.S. Nair, D. Chandran, V.M. Anandakumar, K. Rajendra Babu, Structure and room-temperature ferromagnetism evolution of Sn and Mn-doped NiO synthesized by a sol-gel process, Ceram. Int. 43 (2017) 11090–11096, https://doi.org/10.1016/j.ceramint.2017.05.155.

[21] I.M. Chan, F.C. Hong, I.M. Chan, F.C. Hong, Thin Solid Films 450 (2004) 304e11 Google Search, (n.d.) https://www.google.com/search?q=I.M.+Chan,+F.C.+Hong+Thin+Solid+Films+450+(2004)+304e11.&tbm=isch&source=univ&hl=en&sa=X&ved=2ahUKEwjcs–zrsDhAhXJdd8KHedRCCwQsAR6BAgGEAE&biw=735&bih=746 (accessed April 8, 2019).

[22] K.H. Kim, C. Takahashi, T. Okubo, Y. Abe, M. Kawamura, Influence of NiO anode buffer layer prepared by solution on performance of bulk-heterojunction solar cells, Appl. Surf. Sci. 258 (2012) 7809–7812, https://doi.org/10.1016/j.apsusc.2012.04.017.

[23] R. Kumar, C. Baratto, G. Faglia, G. Sberveglieri, E. Bontempi, L. Borgese, Tailoring the textured surface of porous nanostructured NiO thin films for the detection of pollutant gases, Thin Solid Films 583 (2015) 233–238, https://doi.org/10.1016/j.tsf.2015.04.004.

[24] C.-C. Wu, C.-F. Yang, Fabricate Heterojunction Diode by Using the Modified Spray Pyrolysis Method to Deposit Nickel–Lithium Oxide on Indium Tin Oxide Substrate, (2013) https://pubs.acs.org/doi/abs/10.1021/am400763m (accessed April 8, 2019).

[25] A.C. Nwanya, S.U. Offiah, I.C. Amaechi, S. Agbo, S.C. Ezugwu, B.T. Sone, R.U. Osuji, M. Maaza, F.I. Ezema, Electrochromic and electrochemical supercapacitive properties of room temperature PVP capped Ni(OH)2/NiO thin films, Electrochim. Acta 171 (2015) 128–141, https://doi.org/10.1016/j.electacta.2015.05.005.

[26] Y. Akaltun, T. Cayir, Fabrication and characterization of NiO thin films prepared by SILAR method, J. Alloy. Compd. 625 (2015) 144–148, https://doi.org/10.1016/j.jallcom.2014.10.194.

[27] S.U. Offiah, M.O. Nwodo, A.C. Nwanya, S.C. Ezugwu, S.N. Agbo, P.U. Ugwuoke, R.U. Osuji, M. Malik, F.I. Ezema, Effects of post-thermal treatments on morphological and optical properties of NiO/Ni(OH)2 thin films synthesized by solution growth, Optik 125 (2014) 2905–2908, https://doi.org/10.1016/j.ijleo.2013.11.073.

[28] M.Z. Sialvi, R.J. Mortimer, G.D. Wilcox, A.M. Teridi, T.S. Varley, K.U. Wijayantha, C.A. Kirk, Electrochromic and colorimetric properties of Nickel (II) oxide Thin films prepared by aerosol-assisted chemical vapor deposition, ACS Appl. Mater. Interfaces 5 (2013) 5675–5682.

[29] F.I. Ezema, A.B.C. Ekwealor, R.U. Osuji, Optical properties of chemical bath deposited nickel oxide (NiOx) thin films, Superficies y Vacío 21 (2008) 6–10 http://www.scielo.org.mx/scielo.php?script=sci_abstract&pid=S1665-35212008000100002&lng=es&nrm=iso&tlng=pt (accessed November 30, 2018).

[30] Y.A.K. Reddy, A.M. Reddy, A.S. Reddy, P.S. Reddy, Preparation and Characterization of NiO Thin Films by DC Reactive Magnetron Sputtering, (2012) http://essuir.sumdu.edu.ua/handle/123456789/30257 (accessed April 8, 2019).

[31] K.H. Kim, C. Takahashi, Y. Abe, M. Kawamura, Effects of Cu doping on nickel oxide thin film prepared by sol–gel solution process, Optik 125 (2014) 2899–2901, https://doi.org/10.1016/j.ijleo.2013.11.074.

[32] X. Chen, L. Zhao, Q. Niu, Electrical and optical properties of p-type Li,Cu-codoped NiO thin films, J. Electron. Mater. 41 (2012) 3382–3386, https://doi.org/10.1007/s11664-012-2213-4.

[33] S.C. Chen, T.Y. Kuo, Y.C. Lin, H.C. Lin, Preparation and properties of p-type transparent conductive Cu-doped NiO films, Thin Solid Films 519 (2011) 4944–4947, https://doi.org/10.1016/j.tsf.2011.01.058.

[34] S. Moghe, A.D. Acharya, R. Panda, S.B. Shrivastava, M. Gangrade, T. Shripathi, V. Ganesan, Effect of copper doping on the change in the optical absorption behaviour in NiO thin films, Renew. Energy 46 (2012) 43–48, https://doi.org/10.1016/j.renene.2012.02.028.

[35] P. Scherrer, Bestimmung der inneren Struktur und der Größe von Kolloidteilchen mittels Röntgenstrahlen, in: R. Zsigmondy (Ed.), Kolloidchemie Ein Lehrbuch, Springer Berlin Heidelberg, Berlin, Heidelberg, 1912, pp. 387–409, , https://doi.org/10.1007/978-3-662-33915-2_7.

[36] J.I. Langford, A.J.C. Wilson, Scherrer after sixty years: a survey and some new results in the determination of crystallite size, J. Appl. Crystallogr. 11 (1978) 102–113, https://doi.org/10.1107/S0021889878012844.

[37] 新井敏弘, T.S. Moss, G.J. Burrell, B. Ellis, Semiconductor Opto-Electronics, Butterworths, London, 1973, pp. 874–875 441ページ, 23×15cm, 8,750円., 日本物理學會誌. 28 (1973) https://ci.nii.ac.jp/naid/110002072832/ (accessed April 8, 2019).

[38] E.I. Ugwu, D.U. Onah, Optical characteristics of chemical bath deposited CdS thin film characteristics within UV, visible, and NIR radiation", Pac. J. Sci. Technol. 8 (1) (2007) 155–161.

[39] A.Y. Fasasi, B.D. Ngom, J.B. Kana-Kana, R. Bucher, M. Maaza, C. Theron, U. Buttner, Synthesis and characterisation of Gd-doped BaTiO3 thin films prepared by laser ablation for optoelectronic applications, J. Phys. Chem. Solids 70 (2009) 1322–1329, https://doi.org/10.1016/j.jpcs.2009.06.022.

[40] Waheed Khan, Qun Wang, Xin Jin, Tangfeng Feng, Materials 10 (217) (2017) 1–20 Google Search, (n.d.) https://www.google.com/search?q=Waheed+Khan+,+Qun+Wang+,+Xin+Jin+and+Tangfeng+Feng+Materials++10,+217,+(2017)+1-20&tbm=isch&source=univ&hl=en&sa=X&ved=2ahUKEwj9m-Psu8DhAhVqh-AKHZqZAKIQsAR6BAgJEAE&biw=735&bih=746#imgrc=ud03-XEEVsyo7M (accessed April 8, 2019).

[41] S. Kumar, Y.J. Kim, B.H. Koo, C.G. Lee, Structural and magnetic properties of Ni doped CeO2 nanoparticles, J. Nanosci. Nanotechnol. 10 (2010) 7204–7207.

[42] M. Aliahmad, A. Rahdar, F. Sadeghfar, S. Bagheri, M.R. Hajinezhad, Synthesis and Biochemical effects of magnetite nanoparticle by surfactant-free electrochemical method in an aqueous system:the current density effect, Nanomed. Res. J. 1 (2016) 39–46, https://doi.org/10.7508/nmrj.2016.01.006.

[43] P.A. Hartley, G.D. Parfitt, L.B. Pollack, The role of the van der Waals force in the agglomeration of powders containing submicron particles, Powder Technol. 42 (1985) 35–46, https://doi.org/10.1016/0032-5910(85)80036-X.

[44] H. Wang, X. Kou, L. Zhang, J. Li, Size-controlled synthesis, microstructure and magnetic properties of Ni nanoparticles, Mater. Res. Bull. 43 (2008) 3529–3536, https://doi.org/10.1016/j.materresbull.2008.01.012.

[45] A.C. Nwanya, D. Obi, R.U. Osuji, R. Bucher, M. Maaza, F.I. Ezema, Simple chemical route for nanorod-like cobalt oxide films for electrochemical energy storage applications, J. Solid State Electrochem. 21 (2017) 2567–2576, https://doi.org/10.1007/s10008-017-3520-8.

[46] A.C. Nwanya, M.M. Ndipingwi, N. Mayedwaa, L.C. Razanamahandry, C.O. Ikpo, T. Waryo, S.K.O. Ntwampe, E. Malenga, E. Fosso-Kankeu, F.I. Ezema, Maize (Zea mays L.) fresh husk mediated biosynthesis of copper oxides: potentials for pseudo capacitive energy storage, Electrochim. Acta 301 (2019) 436–448.